

CPNA-1, a copine domain protein, is located at integrin adhesion sites and is required for myofilament stability in *Caenorhabditis elegans*

Adam Warner^{a,*}, Ge Xiong^{b,*}, Hiroshi Qadota^b, Teresa Rogalski^a, A. Wayne Vogl^c, Donald G. Moerman^a, and Guy M. Benian^b

^aDepartment of Zoology and ^cDepartment of Cellular and Physiological Sciences, University of British Columbia, Vancouver, BC V6T 1Z4, Canada; ^bDepartment of Pathology, Emory University, Atlanta, GA 30322

ABSTRACT We identify *cpna-1* (F31D5.3) as a novel essential muscle gene in the nematode *Caenorhabditis elegans*. Antibodies specific to copine domain protein atypical-1 (CPNA-1), as well as a yellow fluorescent protein translational fusion, are localized to integrin attachment sites (M-lines and dense bodies) in the body-wall muscle of *C. elegans*. CPNA-1 contains an N-terminal predicted transmembrane domain and a C-terminal copine domain and binds to the M-line/dense body protein PAT-6 (actopaxin) and the M-line proteins UNC-89 (obscurin), LIM-9 (FHL), SCPL-1 (SCP), and UNC-96. Proper CPNA-1 localization is dependent upon PAT-6 in embryonic and adult muscle. Nematodes lacking *cpna-1* arrest elongation at the twofold stage of embryogenesis and display disruption of the myofilament lattice. The thick-filament component myosin heavy chain MYO-3 and the M-line component UNC-89 are initially localized properly in *cpna-1*-null embryos. However, in these embryos, when contraction begins, MYO-3 and UNC-89 become mislocalized into large foci and animals die. We propose that CPNA-1 acts as a linker between an integrin-associated protein, PAT-6, and membrane-distal components of integrin adhesion complexes in the muscle of *C. elegans*.

Monitoring Editor

Jeffrey D. Hardin
University of Wisconsin

Received: Jun 25, 2012

Revised: Dec 17, 2012

Accepted: Dec 21, 2012

INTRODUCTION

Sarcomeres—highly ordered assemblages of several hundred proteins—perform the work of muscle contraction. Despite ever-increasing knowledge of the components and functions of individual sarcomere proteins, we do not understand how sarcomeres are assembled during development or maintained during muscle contraction. The nematode *Caenorhabditis elegans* is an excellent model genetic system in which to study sarcomere assembly and maintenance (Waterston, 1988; Moerman and Fire, 1997; Moerman and Williams, 2006). In addition to being an excellent system in which to carry out mutational analysis in a whole organism through forward

and reverse genetics, this organism offers several advantages for studying striated muscle. Two advantages of particular note are its optical transparency and its mode of reproduction. The transparency of the nematode allows for evaluation of sarcomere structure by polarized light (Epstein *et al.*, 1974; Waterston *et al.*, 1980; Zengel and Epstein, 1980) and visualization of green fluorescent protein (GFP)-tagged proteins (e.g., Hobert *et al.*, 1999; Meissner *et al.*, 2011). Because the nematode can propagate as a self-fertilizing hermaphrodite, many muscle mutants can be maintained even though these mutants are unable to mate.

Two major integrin adhesion complexes are responsible for building a functional sarcomere in *C. elegans* body-wall muscle: the dense body and the M-line. Prominent proteins in these complexes are α and β integrin (PAT-2, PAT-3; Gettner *et al.*, 1995), kindlin (UNC-112; Rogalski *et al.*, 2000), PINCH (UNC-97; Hobert *et al.*, 1999), integrin-linked kinase (ILK, PAT-4; Mackinnon *et al.*, 2002), and actopaxin (PAT-6; Lin *et al.*, 2003). Another essential protein, vinculin (DEB-1), occurs only within dense bodies (Barstead and Waterston, 1991), and the giant protein UNC-89 occurs solely within M-lines (Benian *et al.*, 1996). The Z-disk analogue in *C. elegans* body-wall muscle is the dense body, an array of proteins anchored by the PAT-2/PAT-3 integrin heterodimer to the muscle cell

This article was published online ahead of print in MBoC in Press (<http://www.molbiolcell.org/cgi/doi/10.1091/mbc.E12-06-0478>) on January 2, 2013.

*These authors contributed equally to this work and are listed alphabetically.

Address correspondence to: Guy Benian (pathgb@emory.edu).

Abbreviations used: *cpna*, copine domain atypical; GFP, green fluorescent protein; GST, glutathione S-transferase; MBP, maltose-binding protein; Pat, paralyzed arrested at twofold; YFP, yellow fluorescent protein.

© 2013 Warner *et al.* This article is distributed by The American Society for Cell Biology under license from the author(s). Two months after publication it is available to the public under an Attribution–Noncommercial–Share Alike 3.0 Unported Creative Commons License (<http://creativecommons.org/licenses/by-nc-sa/3.0>).

“ASCB®,” “The American Society for Cell Biology®,” and “Molecular Biology of the Cell®” are registered trademarks of The American Society of Cell Biology.

membrane, which is responsible for anchoring thin filaments composed mainly of actin. The M-line anchors myosin heavy chain-containing thick filaments and is structurally similar to a dense body but lacks the actin-anchoring proteins DEB-1 (vinculin) and ATN-1 (α -actinin; Francis and Waterston, 1991). Each of these integrin adhesion complexes is needed to transmit the force generated by muscle contraction into movement of the worm.

The aforementioned adhesion proteins are required in body-wall muscle in *C. elegans* to initiate sarcomere assembly and for muscle to function properly. In wild-type animals, at ~420–460 min into development, the embryo elongates to the 1.5-fold stage of embryogenesis and muscle contraction begins (Williams and Waterston, 1994). As the embryo elongates further to the point at which it is folded over on itself, called the twofold stage, movement within the eggshell increases (Williams and Waterston, 1994). In animals lacking one or more essential adhesion complex proteins, embryos arrest elongation at the twofold stage of embryonic development and are paralyzed (Williams and Waterston, 1994), a phenotype unique to defects in embryonic myofilament lattice assembly and contraction in *C. elegans*. Early work on β -integrin (PAT-3; Gettner *et al.*, 1995) and kindlin (UNC-112; Rogalski *et al.*, 2000) in *C. elegans* first implicated these proteins as key molecules in muscle assembly and maintenance. The worm has continued to be a valuable model organism for identification and study of genes required for early steps in muscle assembly (reviewed in Moerman and Williams, 2006). The similarity of dense body and M-line assembly to the formation of adhesion complexes present in tissue culture cells has been reviewed in Cox and Hardin (2004) and Moerman and Williams (2006).

In addition to the essential components for initiating sarcomere assembly, the sarcomere contains a number of extraordinarily large polypeptides (700,000 Da to 4 MDa) composed of multiple copies of immunoglobulin (Ig) and fibronectin type 3 (Fn3) domains, one and even two protein kinase domains, and, in some proteins, elastic regions. In general, these giants are considered to present multiple binding sites, help organize other proteins into the sarcomere, and participate in signaling (Kontrogianni-Konstantopoulos *et al.*, 2009). One of these giant proteins is UNC-89, first identified in *C. elegans* (Waterston *et al.*, 1980; Benian *et al.*, 1996). The human homologue of UNC-89 is obscurin (Bang *et al.*, 2001; Young *et al.*, 2001; Kontrogianni-Konstantopoulos *et al.*, 2009). In *C. elegans* UNC-89 is localized to the M-line (Benian *et al.*, 1996; Small *et al.*, 2004). Loss-of-function mutations in *unc-89* result in worms that display reduced locomotion and disorganized myofibrils, especially at the A-band, and usually lack or display reduced M-lines (Waterston *et al.*, 1980; Benian *et al.*, 1999). Within the myofibril the myosin is disorganized in *unc-89* mutants (Qadota *et al.*, 2008a).

We sought to identify novel proteins involved in sarcomere assembly. We used two approaches: one was an RNA interference (RNAi) screen for new paralyzed arrested at twofold (Pat) mutants (Meissner *et al.*, 2009); the other was a yeast two-hybrid screen for new binding partners of UNC-89. Using these two approaches in parallel, we identified the same protein, copine domain protein atypical-1 (CPNA-1), which contains a copine domain.

RESULTS

F31D5.3/CPNA-1 is an “atypical” copine domain-containing protein

From existing Serial Analysis of Gene Expression libraries, we determined that *cpna-1* is significantly enriched or specific to body-wall muscle (Meissner *et al.*, 2009). From an RNAi screen of ~3300 genes known to be expressed in muscle, we identified *cpna-1* in *C. elegans*

as one of four new Pat mutants (gene model shown in Figure 1A). We examined the phenotype of an intragenic deletion, and likely null mutation, for *cpna-1*, *gk266*, provided by the *C. elegans* Gene Knockout Consortium. The phenotype of worms homozygous for the *gk266* allele is Pat, identical to the RNAi phenotype.

CPNA-1 is most similar to homologues in other nematodes, but CPNA-1 is also similar to mammalian copines. An alignment of CPNA-1 with human copine V isoform CRA_d and a copine domain-containing protein (UniProt entry Q8BIJ1) in the mouse—its two closest homologues in those species (highest BLAST hits)—is shown in Figure 1B using Clustal W (Larkin *et al.*, 2007). Copine domains (Pfam entry PF07002; InterPro entry IPRO10734), also known as von Willebrand A-like or A domains, are ~180 residues long and have weak homology to the extracellular A domain of integrins. Within the copine domain, five key conserved residues (D x S x S ... T ... D) constitute the metal ion-dependent adhesion site (MIDAS), which is found in integrins and copines and is believed to confer functionality to the protein upon association with metal ions (Lee *et al.*, 1995; Whittaker and Hynes, 2002). Copine domains have an unknown function, although they are considered to be cytoplasmic and involved in protein-protein interactions (Tomsig and Creutz, 2002).

All previously characterized proteins containing copine domains also have two C2 domains, which are calcium-dependent phospholipid-binding motifs. Although CPNA-1 does not have predicted C2 domains, multiple online programs predict that CPNA-1 has a transmembrane domain. Each of the programs strongly predicts a transmembrane helix in the N-terminal region, with, for example, TMHMM2.0 (Sonnhammer *et al.*, 1998; Krogh *et al.*, 2001) predicting the region to be residues 23–45. (The closest mammalian homologues of CPNA-1 shown in Figure 1B do not contain predicted transmembrane regions.) Of interest, whereas CPNA-1 shares homology with copine domain-containing proteins in a diverse range of species, including humans, mice, *Arabidopsis*, and *Dictyostelium*, there do not appear to be any homologues in *Drosophila*. Our BLAST search of the *C. elegans* genome revealed that *C. elegans* has seven genes that encode proteins containing copine domains (Figure 2). When compared with CPNA-1, other copine domains in *C. elegans* share 28–55% identity. There is little homology outside of the copine domains, or C2 domains when present, among them. Of the seven genes, only *nra-1* (Gottschalk *et al.*, 2005) and *gem-4* (Church and Lambie, 2003) encode proteins that also contain C2 domains. Thus we designated F31D5.3 as CPNA-1 and call it and the four other copine domain proteins that lack C2 domains “copine domain atypical,” with gene designations *cpna-1* through *cpna-5*, respectively.

CPNA-1 localizes to dense body and M-line muscle integrin adhesion complexes and is required for maintenance of muscle stability

To determine the localization of CPNA-1 in nematode muscle, we raised antibodies to a non-copine-domain region of CPNA-1 (Figure 1A). These antibodies detected a single band on a Western blot using a protein lysate from *C. elegans* (Supplemental Figure S1). The size of this band, ~130 kDa, is very similar to the size of the predicted CPNA-1b isoform. Anti-CPNA-1 antibodies were used to visualize CPNA-1 localization in wild-type adult body-wall muscle. As shown in Figure 3A, CPNA-1 localizes to both M-lines and dense bodies, colocalizing with UNC-89 (M-lines), and with α -actinin (dense bodies). In *cpna-1* (*gk266*) animals we do not observe any CPNA-1 staining, indicating the mutation is likely a null. UNC-112 (kindlin) is located at M-lines and dense bodies (Rogalski *et al.*, 2000) and has been shown to interact with the cytoplasmic tail of PAT-3

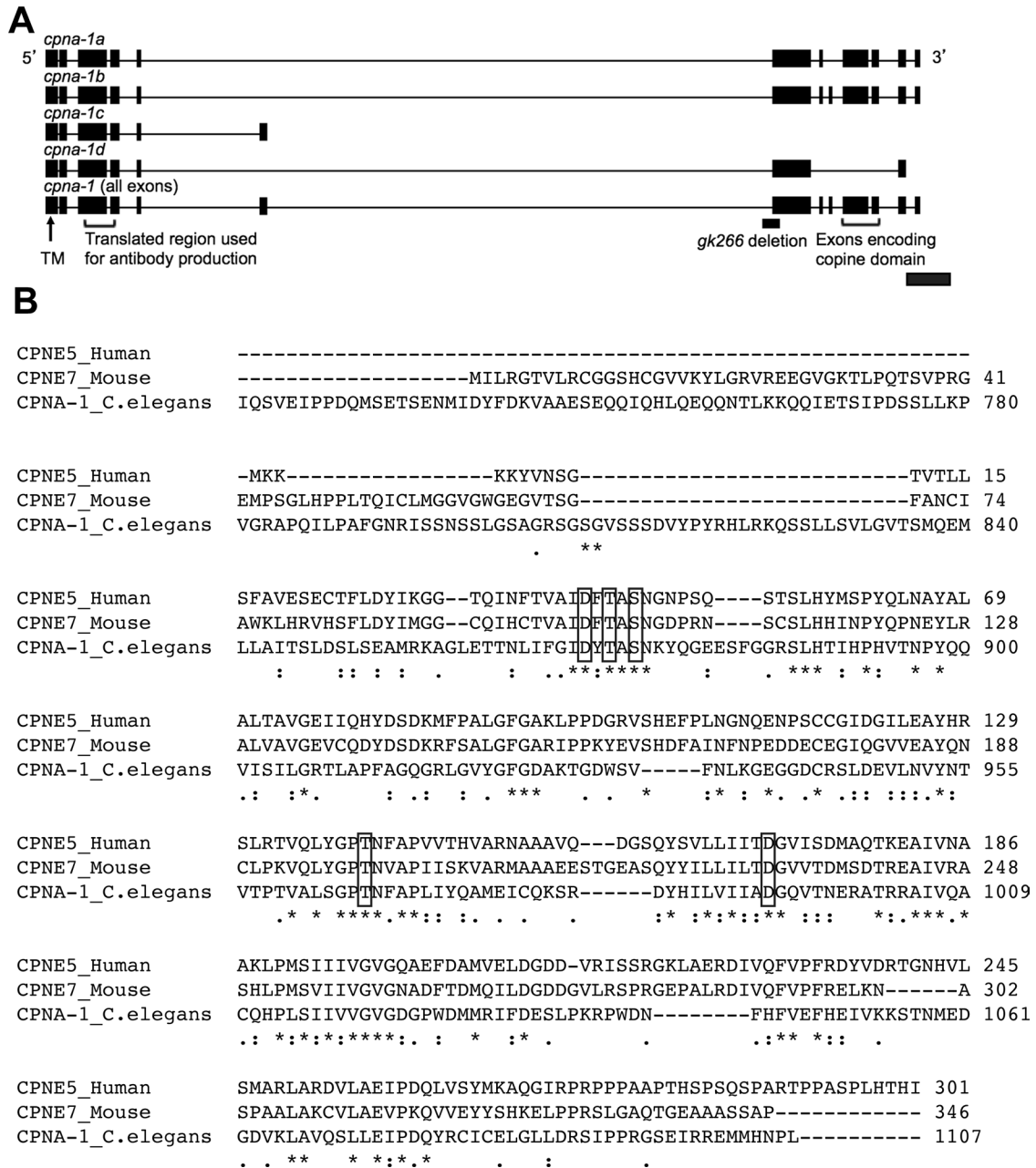
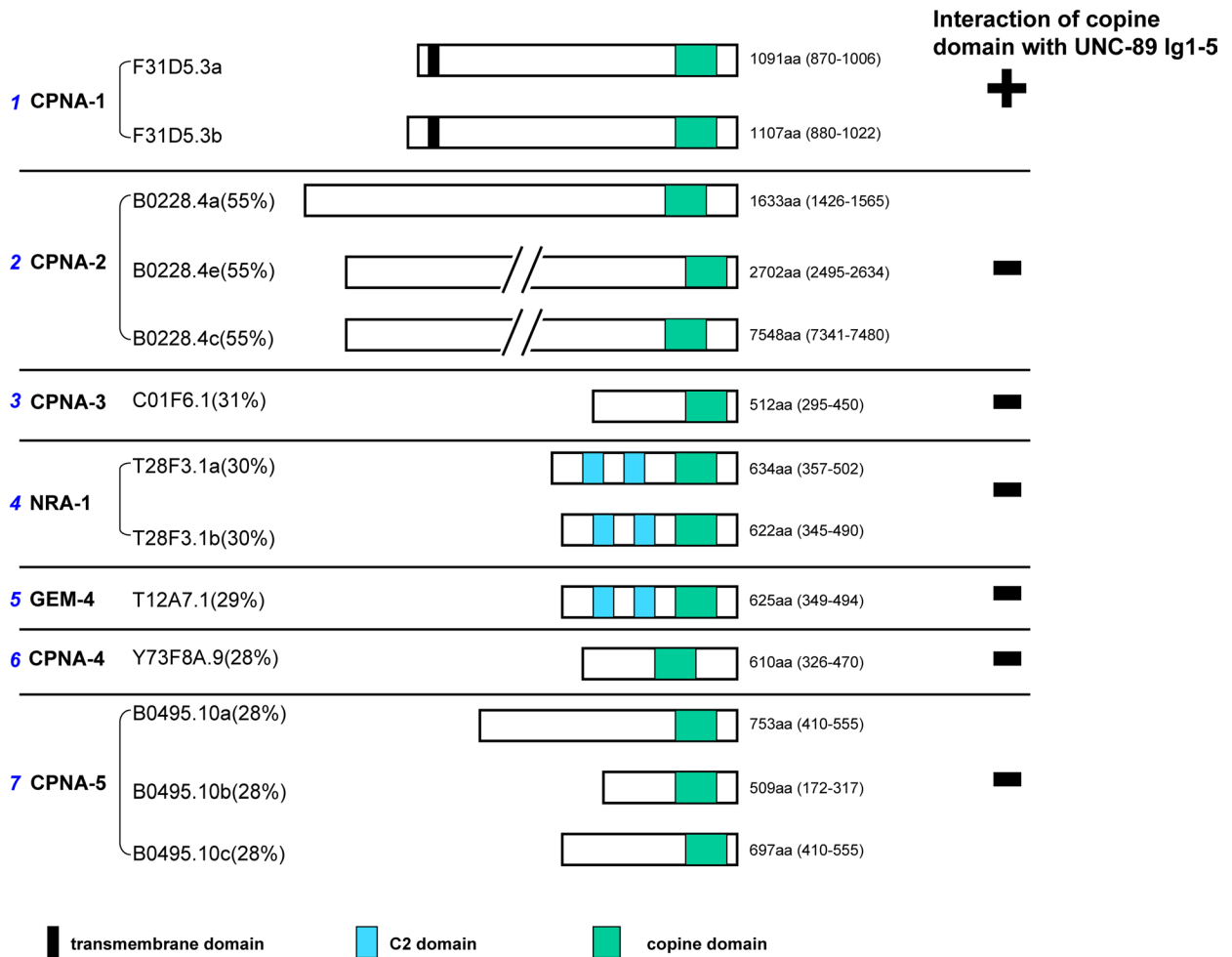


FIGURE 1: Gene model for *cpna-1* and alignment of CPNA-1 with human and mouse homologues. (A) Exon–intron organization of the *cpna-1* gene; thin lines, introns; thick black boxes, exons. The last row includes all the exons, with labeling of key features of the gene or protein. *cpna-1* has four predicted splice isoforms, with the largest isoform (isoform b) spanning 21,834 nucleotides. *cpna-1b* codes for a protein of 1107 amino acids and contains a predicted amino-terminal transmembrane domain and a carboxy-terminal copine domain. The *gk266* allele has a 9–base pair insertion at the 3′ end of intron 5, followed by a 393–base pair deletion that extends into the 5′ end of exon 6. Regions used for antibody production and coding for the predicted transmembrane domain (TM) and copine domain are indicated. The black bar at the bottom right represents 1 kb. (B) When aligned with human and mouse homologues, CPNA-1 does not align at its amino terminus due to its longer length, but there is strong conservation among all of the proteins in the copine domain and surrounding region. In addition, key residues of a MIDAS site are conserved in each aligned protein and are indicated by open rectangles. Asterisks indicate identical amino acids, colons indicate conserved substitutions, and periods indicate semiconserved substitutions.

(β-integrin; Qadota *et al.*, 2012). Thus UNC-112 can be considered as a marker for proteins that are located close to the muscle cell membrane. Anti-CPNA-1 antibodies were used to stain transgenic animals expressing GFP-tagged UNC-112. As shown in Figure 3A (third row), CPNA-1 colocalizes with the membrane proximal protein

UNC-112, and therefore CPNA-1 is membrane proximal in both dense bodies and M-lines. In addition, we costained for CPNA-1 and one more membrane-proximal component, PAT-6 (actopaxin), which is a member of the conserved four-protein complex that associates with the cytoplasmic tail of PAT-3 (β-integrin; Lin *et al.*,

A**B**

```

1  SLHTIHPHVTNPY--QQVVISLGRTLAPFAG--QGRLGVYGF*GDAKTGDWSVFNLKGE---|CPNA-1
1  PLHTIDPAEMNPY--QQVIQIVGKTLSSFDA--DGQIPAYGFGDEEFTDHGIFNIAERYDL|CPNA-2
1  SLHYIHPHQSPYLEALLQTVPPLLAYLPNPQNPHIGALGFGAKVQVPGGALQLSHCFCL|CPNA-3
1  SLHFMSADRPNQY-ELALRSVLSICQHYSN--SKTFEAFGFGAKLPNQ---SSVSAIFPL|NRA-1
1  SLHYMATGIPNQY-EIALRSVLTICQHYSN--SKTFEAFGFGAKLPNH---QTVSAVFPPL|GEM-4
1  -MDY--QQYSNDI-EFVVRSLGDTLEPFNP--TNSWLSYGF*GAKIPPH---YRDSNNEFCL|CPNA-4
1  -----FGIGAKIPPT---FHESNEFFL|CPNA-5
   slh      n y e      v l      GfGak p      s f l consensus

55  ----GGDCRS*LDV*LVN*YNTVTPVALSGPTNFAPLIY----QAMEICQKS---RDYH|CPNA-1
58  ----EKDCNGFEEVLRVYNEVTPTEIEMSGPTNFVPLID----RAIEICKEK---HSYH|CPNA-2
61  NGTPTDPRVEGLGGLLSAYRTAVMGLQFPAPTD*SEVIYFMSKFAKESRRHV---GLYF|CPNA-3
55  DLQRGTSEVVGITGVMTAYRHALSNVQLYGPTNFAPIIENVAR-KAQNMIHDS---ARYQ|NRA-1
55  DLNRQSSSVVINGVMNAYRHALQNVTLYGPTNFSP*IIVEVAN-KAQKMMKTT---ARYQ|GEM-4
52  SLD-ADATCGVNGV*LGAFKSHQHVHPLSGAKFSQIIYHLAK-QAQN*NFN*RANEP*PSY*|CPNA-4
20  NFS-MDPICRGLDGVMEAYRKTQTMVTPLKESKLS*SPVINYVTR-MSHRSGFRG---LHYH|CPNA-5
   g gvl ayr      v      gptnfs p I      a      Y consensus

102  ILLV*IADG---QVTNERATRR*AI*VQACQHPLSII*VVGVG|CPNA-1
105  ILLV*IADG---QVTNEKINQKAI*AAASHYPLSII*IMVGVG|CPNA-2
118  VLI*IYSDGGPANALNMKRSIDAI*VDSAPHMSII*IGVGMG|CPNA-3
111  ILLI*ITDG---IISDMHATIRS*IISASGLPLSIII*IGV|NRA-1
111  ILLI*ITDG---IISDMYATINTVINASGLPLSIII*IGV|GEM-4
110  VLI*ITRG---SIEDLKETVQA*AIFASKAPISIV*FGV|CPNA-4
75  VIALFTRG---EVTDLKEIQALNSA*SDAPLSILI*IGMG|CPNA-5
   iL iitdG      d      ai As PLSII vGvG consensus

```

FIGURE 2: Copine family proteins in *C. elegans*. (A) The *C. elegans* genome has seven genes (1–7) that encode proteins containing copine domains. The protein names shown are based on gene names (e.g., CPNA-1) and sequence names (e.g., F31D5.3). Percentages refer to the percentage of identical amino acid residues in each copine domain as compared with the copine domain of CPNA-1. The numbers in parentheses after the total number of amino acid residues in each protein denote the positions of copine domains. Note that only NRA-1 and GEM-4 are “typical,” in that they also contain C2 domains. Only CPNA-1 also has a predicted transmembrane domain. In addition, some isoforms of CPNA-1 and CPNA-2 are not shown. These isoforms, predicted on WormBase (CPNA-1c, CPNA-1d, CPNA-2b, and

2003). As shown in Figure 3A (last row), CPNA-1 and PAT-6 colocalize to both dense bodies and M-lines.

As described previously, worms lacking *cpna-1* due to either mutation or RNAi arrest elongation at the twofold stage of embryogenesis and die as abnormal L1 larvae. As shown in Figure 4A, whereas a wild-type worm hatches and progresses normally to the first larval stage, *cpna-1(gk266)* homozygotes (Figure 4B) arrest elongation during embryogenesis. In an attempt to rescue the embryonic lethal phenotype, we constructed a yellow fluorescent protein (YFP) translational fusion. The recombinered fosmid fDM1217 did not successfully rescue the lethal phenotype; however, YFP-tagged CPNA-1 localizes to dense bodies and M-lines (Figure 4C) in a pattern identical to that seen with our CPNA-1 immunostaining. Colocalization with PAT-3 staining (Figure 4D) is shown in Figure 3E. The localization pattern of CPNA-1::YFP is similar to that of PAT-3 in dense bodies and M-lines, and it is also seen more broadly around the dense bodies when compared with the localization pattern of PAT-3.

It is clear that CPNA-1 is located at dense bodies and M-lines, but its position vis-à-vis the plasma membrane needed to be clarified. We took two approaches to address this question. We did a confocal Z-series beginning at the plasma membrane and extending into the cell at 0.5- μ m increments (see Supplemental Figure S2). We see that CPNA-1 is close to the plasma membrane, at the same level as the ECM protein UNC-52 (perlecan) and the membrane-proximal proteins UNC-112 and PAT-6, but also extends more deeply into the cell than these proteins. However, CPNA-1 does not extend as deeply into the cell as the M-line protein UNC-89 (obscurin).

We also examined transmission electron microscopy (TEM) sections of CPNA-1::YFP animals using colloidal gold-labeled anti-YFP antibodies to determine whether the protein is close to the plasma membrane. In the tested animals, YFP sequence is fused to CPNA-1 at the C-terminal end of the protein, whereas the N-terminal of the protein is predicted to be transmembrane, so we did not expect to see colloidal gold within the plasma membrane even if CPNA-1 does traverse the membrane. We focused on dense bodies rather than M-lines because dense bodies are more visible in TEM images. In worm sections, CPNA-1 labeled with colloidal gold is visible within and surrounding the dense body (Figure 3B, middle) at much higher levels than the random localization of gold particles in control images (Figure 3B, right). We compared the number of gold particles observed within a dense body or directly adjacent to the visible portion of dense bodies in control sections and experimental sections. Control sections had an average of 6 gold particles per dense body, whereas sections with colloidal gold-labeled CPNA-1 had an average of 24.25 gold particles per dense body. CPNA-1 is observed in dense bodies both distal and proximal to the cell membrane (Figure 3B, middle), supporting the idea that some CPNA-1 molecules localize close to or within the basal membrane of body-wall muscle cells at integrin adhesion sites.

CPNA-1 acts to maintain sarcomere integrity

We examined the localization pattern of essential body-wall muscle proteins in the *cpna-1*-mutant background using immunostaining

for each protein tested. For each of PAT-3 (β -integrin; Figure 4G), DEB-1 (vinculin; Figure 4I), PAT-4 (ILK; Figure 4K), and PAT-6 (actopaxin; Figure 4M), each protein was localized at integrin adhesion complexes in muscle quadrants, albeit with some minor disorganization when compared with wild-type embryos. These results are typical when staining embryos for proteins that act earlier in sarcomere assembly than the protein under study (Williams and Waterston, 1994; Norman et al., 2007). These observations indicate that CPNA-1 is not necessary for the earliest steps in sarcomere initiation.

In *cpna-1*-null embryos, UNC-89 (obscurin) is properly localized to adhesion sites before the 1.5-fold stage (Figure 4O), but in later stages (1.75- and 2-fold), UNC-89 is found in abnormal accumulations (Figure 4Q). Similarly, in *cpna-1*-null embryos, MYO-3 is properly organized into discrete sarcomeres before the 1.5-fold stage (Figure 4S), but in later stages (1.75- and 2-fold), MYO-3 is found in abnormal accumulations (Figure 4U). These observations suggest that CPNA-1 is essential to maintain the integrity of both UNC-89 and MYO-3 at muscle integrin adhesion sites, and in *cpna-1*-null animals, elongation arrests due to either the mislocalization of MYO-3 or other factors.

Using anti-CPNA-1 antibodies, we carried out the reciprocal experiment and examined the localization of CPNA-1 in the mutant background of a number of Pat mutants. In *pat-3*-arrested (Figure 5B) and *pat-4*-arrested (Figure 5C) embryos, CPNA-1 is mislocalized, appearing in bright fluorescent patches within the muscle cells (arrows). In *pat-6* embryos (Figure 5, D and E), CPNA-1 shows some variability in its localization, ranging from severe mislocalization (Figure 5D), similar to that seen in the *pat-3* and *pat-4* backgrounds, to proper polarization in the membrane but disorganized (Figure 5E). In contrast, CPNA-1 is localized normally in *myo-3*-arrested embryos (Figure 5F), closely resembling the localization of CPNA-1 in wild-type embryos (Figure 5A). These cumulative results place *cpna-1* between *pat-6* and *myo-3* in the M-line/dense body assembly pathway.

CPNA-1 interacts with UNC-89 and several other muscle integrin adhesion complex proteins

In an effort to identify new binding partners for UNC-89, we used a portion of UNC-89 comprising Ig domains 1–5 (Ig1–5) as bait to screen a yeast two-hybrid library of *C. elegans* cDNAs (Figure 6A). Two positive preys representing CPNA-1 were recovered. The smallest prey clone (residues 825–1058) contains essentially just the copine domain, suggesting that this region of CPNA-1 is minimally required for interaction with UNC-89. CPNA-1 was used in yeast two-hybrid assays as both bait and prey to test for interaction with an additional 16 portions of UNC-89. As indicated in Figure 6B, CPNA-1 (825–1058) interacts only with Ig1–5. Given our understanding of the regulation of the *unc-89* gene (Ferrara et al., 2005), CPNA-1 is predicted to interact with the large UNC-89 isoforms (A, B, E, and F) but not the small isoforms (C and D). When tested by two-hybrid assays against copine domains from each of the seven copine domain-containing proteins, UNC-89 Ig1–5 interacted only with the copine

CPNA-2d), lack copine domains. The rightmost column represents results of yeast two-hybrid assays in which UNC-89 Ig1–5 was tested for interaction with copine domains from each of the seven *C. elegans* genes. +, interaction; –, no interaction. (B) Multisequence alignment of the copine domains in the seven *C. elegans* copine domain proteins. Green shading indicates residues present in all seven copine proteins, and yellow shading indicates residues present in four or more copine proteins. "Consensus" represents the green (uppercase) and yellow (lowercase) shaded residues. Asterisks denote conserved residues that were mutated in the copine domain of CPNA-1 and tested for binding to UNC-89 and UNC-96 (Figure 7).

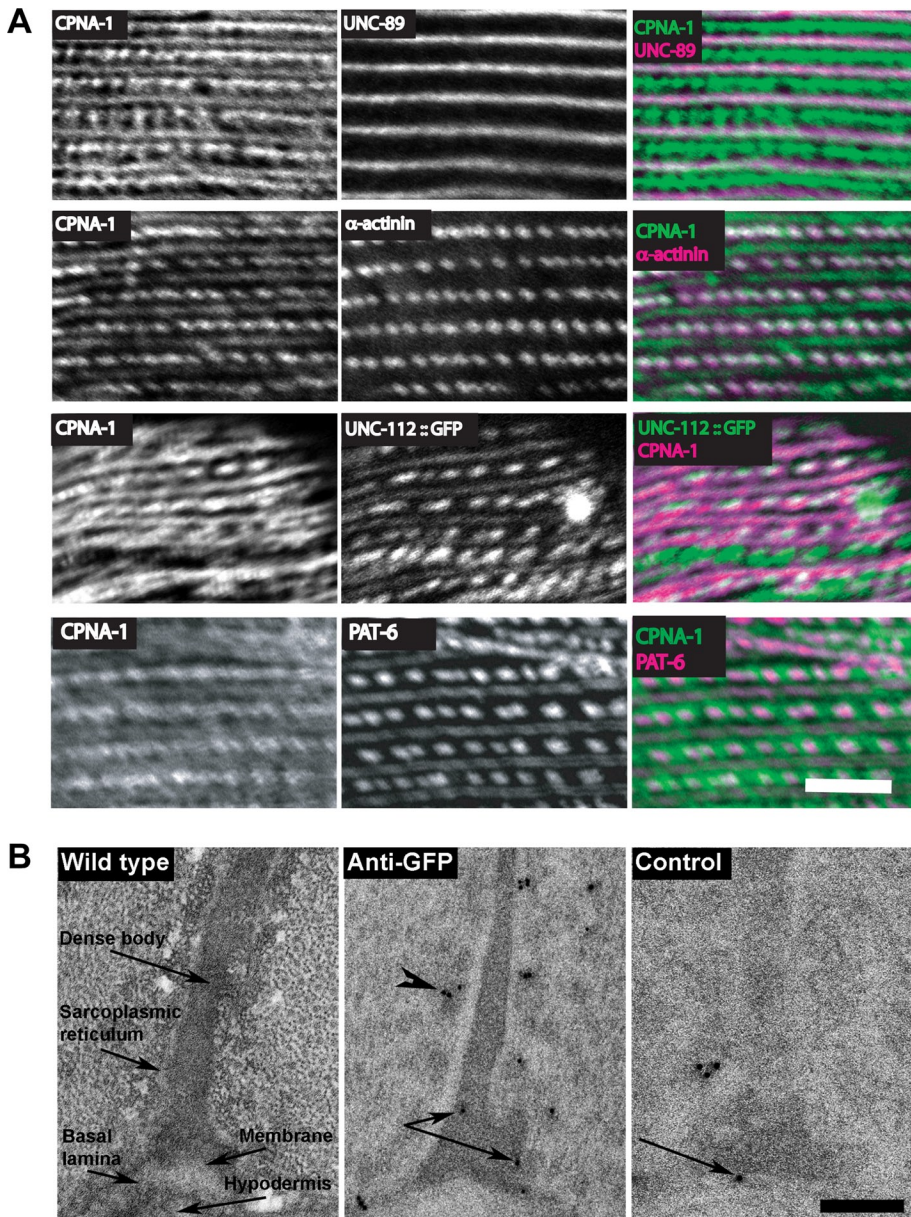


FIGURE 3: Immunolocalization of CPNA-1 to adult muscle M-lines and dense bodies. (A) Wild-type adults were costained with anti-CPNA-1 and anti-UNC-89 (first row) or anti-CPNA-1 and anti- α -actinin (second row); a transgenic line carrying UNC-112::GFP was also stained with anti-CPNA-1 (third row); costaining with CPNA-1 and PAT-6 is shown in the fourth row. CPNA-1 clearly localizes to both M-lines (colocalizing with the M-line protein UNC-89) and dense bodies (colocalizing with the dense body protein α -actinin). At least some CPNA-1 localizes near the muscle cell membrane, since some CPNA-1 colocalizes with the membrane-proximal proteins UNC-112 and PAT-6. Colocalization is indicated by white (overlap of green and magenta). Bar, 10 μ m. (B) Major components of the muscle cell are labeled in the TEM image (left). Thin (small dots) and thick (larger dots) filaments can be observed in the Z-plane to the sides of the dense body. Gold particles (dark black dots) show CPNA-1::YFP within (arrow) and surrounding the dense body (arrowhead; middle). A control TEM section incubated with complete chicken IgY and secondary antibody conjugated with gold particles (right) has random gold localization at much lower levels (arrow). Bar, 100 nm.

domain from CPNA-1 (Figure 2). This is a further indication of the specificity of the UNC-89 to CPNA-1 interaction. Deletion derivatives of Ig1–5 were used in two-hybrid assays against CPNA-1. As shown in Figure 6C, the minimal region necessary and sufficient to interact with CPNA-1 is Ig1–3. Two biochemical approaches were used to verify the interaction of UNC-89 with CPNA-1 (Supplemental Figure S3).

To identify additional CPNA-1 binding partners, we used CPNA-1 to conduct a yeast two-hybrid screen of a collection of 23 known components of dense bodies and M-lines (Supplemental Table S1). As indicated in Figure 6, D–H, we identified four additional CPNA-1–interacting proteins: SCPL-1 (a CTD-type protein phosphatase; Qadota *et al.*, 2008b), LIM-9 (FHL; Qadota *et al.*, 2007), PAT-6 (actopaxin; Lin *et al.*, 2003), and UNC-96 (Mercer *et al.*, 2006). The minimal portions required for interaction with CPNA-1 were also determined. Although only the copine domain of CPNA-1 is required to interact with UNC-96, nearly full-length CPNA-1 is required for interaction with SCPL-1, LIM-9, and PAT-6. These interactions were confirmed using *in vitro* binding experiments with purified proteins (Supplemental Figure S4). Thus CPNA-1 has both dense body and M-line binding partners.

We demonstrated that the copine domain of CPNA-1 can interact with UNC-89 Ig1–5 and with UNC-96 (201–418). We used *in vitro* mutagenesis to test whether CPNA-1 has distinct binding sites for these proteins. Alignment of copine domains from the *C. elegans* proteins reveals 12 invariant amino acid positions (shaded green in Figure 2B), which are also conserved in the PFAM consensus sequence for all copine proteins. We mutated three of the 12 conserved residues (asterisks in Figure 2B): G922 was changed to V, which has a larger side chain and may cause a local conformational change; Y985 to A to alter the side chain; or F, which eliminates a possible phosphorylation site or eliminates hydrogen bonding or even ionic bonding independent of phosphorylation. Similarly, S1015 to A to eliminate a possible phosphorylation site. As shown in Figure 7A, the G922V mutation eliminates only the interaction with UNC-89, and the S1015A mutation eliminates only the interaction with UNC-96, suggesting that the copine domain of CPNA-1 might have distinct binding sites for these two M-line proteins.

Based on our mutant analysis (Figures 4 and 5), PAT-6 is required for assembly of CPNA-1 into integrin adhesion sites, and CPNA-1 is required for the stable association of UNC-89 with integrin adhesion sites. As such, we might expect to obtain evidence that PAT-6, CPNA-1, and UNC-89 form a ternary structure. To test this idea, we performed a yeast three-hybrid assay. UNC-89 Ig1–5 as bait was coexpressed with hemagglutinin (HA)-tagged CPNA-1 (173–1107), or empty vector as control, and PAT-6 as prey. As shown in Figure 7B, the interaction of UNC-89 Ig1–5 with PAT-6 depends on the presence of CPNA-1. This result is consistent with the existence of a ternary

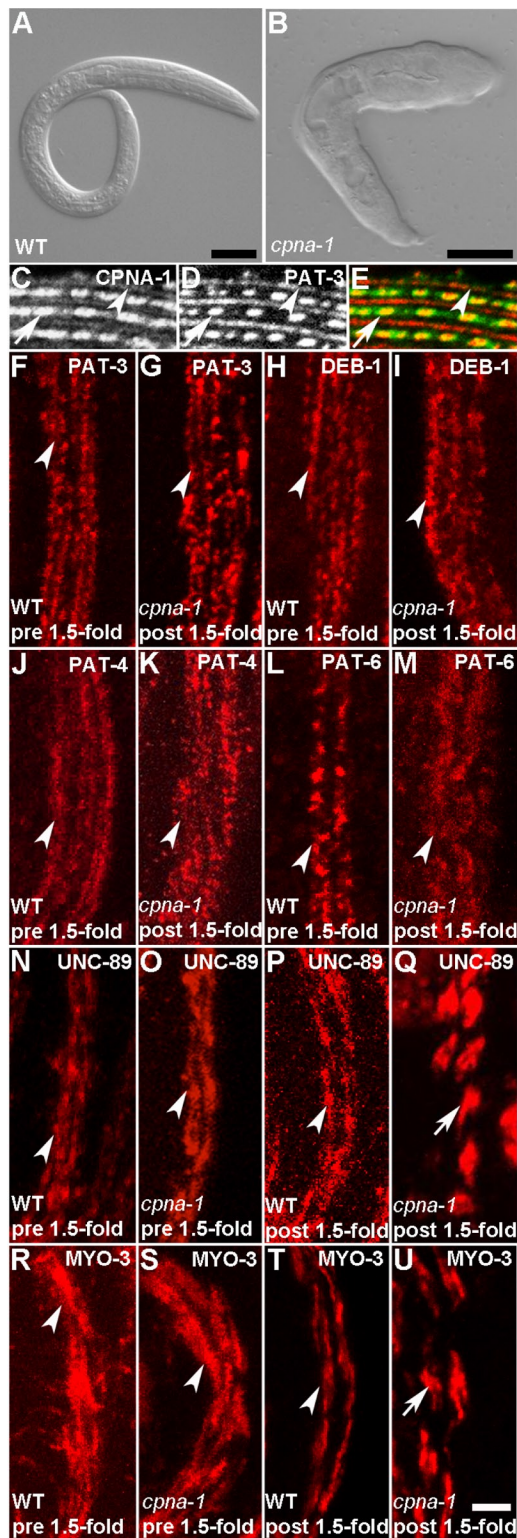


FIGURE 4: Characterization of the *cpna-1*-null phenotype and localization of CPNA-1::YFP in body-wall muscle. Wild-type *C. elegans* proceeds through embryogenesis to hatch as a first-larval-stage animal (A), whereas a *cpna-1*-null animal of the same age arrests elongation at the twofold stage of embryogenesis (B). CPNA-1::YFP is localized to dense body (arrows) and M-line integrin adhesion complexes (arrowheads) in adult body-wall muscle (C). Colocalization of CPNA-1::YFP is observed (E) in worms immunostained for PAT-3 (β -integrin; D), a key constituent of the same integrin adhesion structures. In E note that CPNA-1 is also localized to areas directly

complex containing PAT-6, most of CPNA-1, and a small portion of UNC-89.

The role of CPNA-1 in postembryonic body-wall muscle

Previously we used RNAi on postembryonic-stage animals to investigate whether CPNA-1 was required in body-wall muscle (Meissner *et al.*, 2009). In *cpna-1* (RNAi)-treated adult animals, the arrays of myofilaments in body-wall muscle are highly disorganized, as visualized by polarized light microscopy.

PAT-6 is the earliest protein in the M-line/dense body assembly pathway that interacts with CPNA-1. Our mutant analysis indicates that CPNA-1 is downstream of PAT-6 in embryonic muscle. These results led us to explore the relationship between PAT-6 and CPNA-1 in adult muscle. We used RNAi to knock down *pat-6*, beginning at the L1 larval stage, in order to avoid the embryonic requirement of *pat-6*. In muscle cells with nearly undetectable PAT-6, CPNA-1 was mislocalized, being found in abnormal accumulations (arrowhead) or at the edges of the muscle cell (arrows; Figure 8).

We next did the same experiment with UNC-89, SCPL-1, UNC-96, and LIM-9. None of these four proteins is required for embryonic muscle development, but when deficient, they have phenotypes in adult muscle (Waterston *et al.*, 1980; Mercer *et al.*, 2006; Meissner *et al.*, 2009; Nahabedian *et al.*, 2011). As shown in Figure 9, the localization of CPNA-1 at M-lines (indicated by arrows) is unaffected by the absence or reduced levels of UNC-89, SCPL-1, UNC-96, or LIM-9 in L4 or early- or late-stage adults. These results are consistent with these proteins being downstream of CPNA-1 in the M-line assembly pathway in postembryonic muscle.

DISCUSSION

A model for CPNA-1 in maintenance of integrin adhesion complexes

Our studies identified CPNA-1 as a new component of integrin adhesion complexes, based on four criteria. First, CPNA-1 is localized to M-lines and dense bodies, similar to integrin and integrin-associated proteins (Moerman and Williams, 2006). Second, loss of function of CPNA-1 leads to a Pat embryonic lethal phenotype. This terminal phenotype can result from loss of function of genes encoding integrin and integrin-associated proteins. Third, whereas MYO-3 and UNC-89 are initially localized in *cpna-1*-null embryos, as the embryo proceeds to the twofold stage, both proteins become mislocalized and accumulate at the edges of muscle cells. This demonstrates that CPNA-1 is required for maintaining the

adjacent to the dense body, observed by the green localization pattern around the dense body; stronger M-line staining by PAT-3 (red) overshadows that of CPNA-1 (arrowhead). Compared to wild-type staining (F, H, J, L), when *cpna-1* embryos are immunostained with antisera for PAT-3 (G), DEB-1 (I), PAT-4 (K), and PAT-6 (M), only slight disorganization is seen and each of the four proteins is still localized to the appropriate integrin adhesion sites (arrowheads). In pre-1.5-fold embryos, UNC-89 is able to localize to M-lines in both wild-type embryos (N) and *cpna-1*-null embryos (O), but after the 1.5-fold stage, wild-type embryos (P) show normal UNC-89 localization, whereas *cpna-1*-null embryos show UNC-89 mislocalized into large foci within muscle cells (Q; arrows). Similarly, MYO-3 is able to organize into nascent thick filaments in both pre-1.5-fold wild-type (R) and *cpna-1*-null (S) embryos, but after the 1.5-fold stage, wild-type embryos (T) show normal MYO-3 localization to nascent thick filaments, whereas in *cpna-1*-null embryos, MYO-3 is disorganized and mislocalized into large accumulations within the muscle cells (U; arrows). Bars, (A and B) 20 μ m, (C–U) 2 μ m.

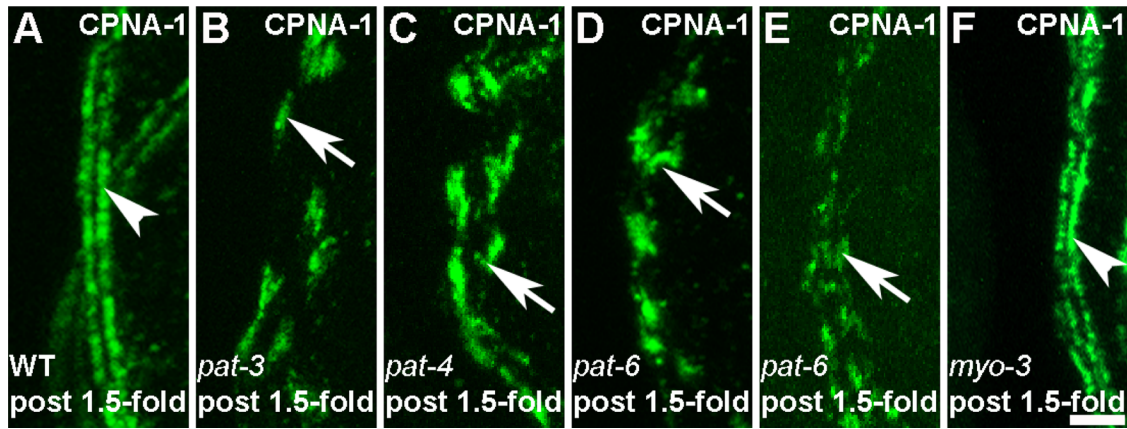


FIGURE 5: Immunolocalization of CPNA-1 in the null background of other Pat genes. In late-stage, wild-type embryos, CPNA-1 is organized into bands of dense bodies and M-lines in the muscle cell quadrants (A; arrowheads). In null *pat-3* embryos, however, CPNA-1 is mislocalized into large aggregates within body-wall muscle cells (B; arrows). Similarly, large accumulations of CPNA-1 are also seen in null embryos for *pat-4* (C) and *pat-6* (D; arrows), although in some *pat-6* embryos, CPNA-1 mislocalized to a lesser extent than for *pat-3* and *pat-4* embryos (E; arrow). In arrested twofold embryos lacking MYO-3, however, CPNA-1 is organized properly into bands of dense bodies and M-lines (F), as it is in wild-type embryos (A, arrowheads). Bar, 2 μ m.

structural stability of thick-filament attachments. Finally, CPNA-1 binds directly to PAT-6, one of the integrin-associated proteins. We suggest that the molecular function of CPNA-1 is to act as a linker between integrin-associated proteins near the muscle cell membrane and proteins that are found deeper inside the muscle cell (Figure 10). In striated muscle of *C. elegans*, both the M-lines and dense bodies are integrin adhesion complexes containing both shared and specific protein components. At the base of each M-line and dense body, associated with the cytoplasmic tail of β -integrin, is a complex of four conserved proteins, including UNC-112 (kindlin), PAT-4 (ILK), UNC-97 (PINCH), and PAT-6 (actopaxin). Lin *et al.* (2003) showed that PAT-4 (ILK) interacts with the C-terminal CH domain of PAT-6 (actopaxin). Here, we show that the N-terminal portion of PAT-6, including the first CH domain, interacts with CPNA-1. CPNA-1, in turn, interacts with UNC-89 (obscurin), LIM-9 (FHL), SCPL-1 (SCP), and UNC-96 at M-lines (Figure 10). We speculate that there are as-yet-unidentified dense body-specific proteins that interact with CPNA-1.

CPNA-1 is not required for the initial assembly of sarcomeric components, but embryonic muscle lacking CPNA-1 becomes disorganized after muscle contraction begins. CPNA-1 binds to PAT-6, UNC-89, and other integrin adhesion complex proteins to possibly hold together the integrin adhesion complex. In this manner, MYO-3 (myosin) and other membrane-distal components of the sarcomere remain in their proper locations, and the sarcomere is stable. In the absence of CPNA-1, the integrin adhesion complex would not be maintained or repaired during the stress of contraction, and the sarcomere would fall apart. Work by Tomsig *et al.* (2003) might support this proposed mode of action. The copine domain of CPNA-1 contains key residues of a MIDAS (Figure 1B), and Tomsig *et al.* (2003) demonstrated that these sites are important for human copines to recruit binding partners in a calcium-dependent manner. Given that muscle contraction is a calcium-regulated process, one could infer that CPNA-1 might be involved in the recruitment of binding partners during contraction and consequently plays a role in maintaining sarcomere integrity. An alternative possibility is that CPNA-1 maintains stability by recycling damaged sarcomere components or acts by recruiting new proteins to the integrin adhesion complexes. In this regard, one could speculate that the predicted transmembrane

domain of CPNA-1 inserts into membrane vesicles and is involved in moving damaged or newly synthesized proteins from or to muscle integrin adhesion complexes.

New classes of copine domain-containing proteins

Copines are evolutionarily conserved proteins found in plants and animals and have been analyzed genetically in *Arabidopsis* (Hua *et al.*, 2001; Jambunathan *et al.*, 2001), *Dictyostelium* (Damer *et al.*, 2007), and *C. elegans* (Church and Lambie, 2003; Gottschalk *et al.*, 2005). Copines were first identified as Ca^{2+} -dependent phospholipid-binding proteins in *Paramecium* (Creutz *et al.*, 1998), contain two C2 domains, and are usually believed to be involved in membrane trafficking. CPNA-1 is the first characterized copine domain-containing protein that lacks C2 domains. The Pfam website (<http://pfam.sanger.ac.uk/>), as of April 2011, notes 200 sequences from diverse organisms that have a copine domain plus two C2 domains, 25 with copine domains plus a single C2 domain, and 168 containing only a copine domain. This copine domain-only category includes an uncharacterized putative protein from the mouse (UniProt entry Q8BIJ1 MOUSE; 346 amino acids) and isoform CRA_d of copine V from humans (UniProt entry Q7Z6C8 HUMAN; 301 amino acids), as shown aligned with CPNA-1 in Figure 1B. These are the two closest homologues to CPNA-1 in those species.

Among the copine domain-containing proteins in the *C. elegans* proteome, both typical and atypical, only CPNA-1 contains a predicted transmembrane domain. In fact, our *in silico* analysis has not revealed any human copine proteins that have a predicted transmembrane domain. Although both confocal (Figure 3A and Supplemental Figure S2) and electron microscopic (Figure 3B) imaging reveal some fraction of CPNA-1 at or near the muscle cell membrane at the base of dense bodies and M-lines, whether this predicted transmembrane domain inserts into this or any other membrane will require additional experiments. Note that our domain mapping (Figure 6F) indicates that the predicted transmembrane domain of CPNA-1 is not required for its association with PAT-6. Thus CPNA-1 might have two ways to localize to integrin adhesion complexes—binding to the integrin-associated protein PAT-6, and direct insertion of its transmembrane domain into the muscle cell membrane.

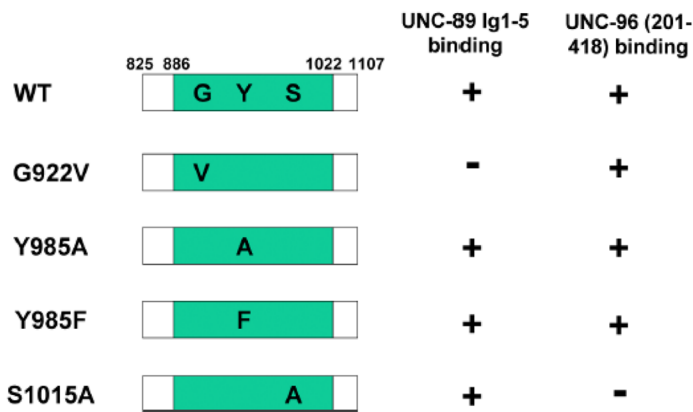
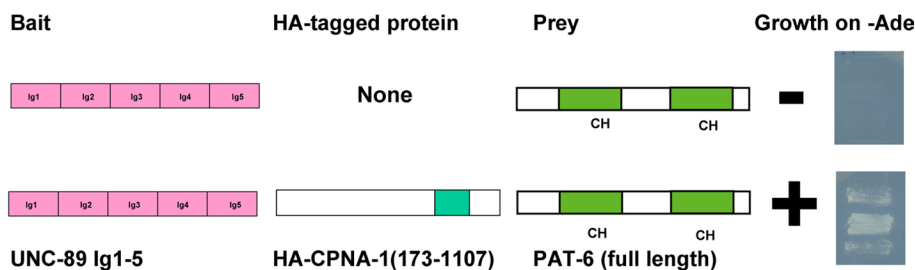
A**B**

FIGURE 7: Point mutations in the copine domain of CPNA-1 affects its binding to UNC-89 and UNC-96; evidence for a ternary complex containing PAT-6 and portions of CPNA-1 and UNC-89. (A) The copine domain of CPNA-1 has distinct binding sites for UNC-89 and UNC-96. Three of the 12 conserved residues of copine domains (indicated with asterisks in Figure 2B) were changed: G922 was changed to V; Y985 was changed to A and F, respectively; S1015 was changed to A. The G922V mutation eliminates binding to UNC-89 but not UNC-96. Similarly, the S1015A mutation eliminates the binding to UNC-96 but not UNC-89. (B) UNC-89 Ig1-5 as bait was coexpressed with HA-tagged CPNA-1 (residues 173–1107; or empty vector as control) and PAT-6 (full length) as prey. +, growth on –Ade plates; –, no growth on –Ade plates. Right, the yeast growth on –Ade plates from each experiment from three independent colonies.

Alternatively, the predicted transmembrane domain might not be involved in localization to the muscle cell membrane but might insert in other membrane compartments, for example, vesicles involved in repair or replacement of sarcomeric proteins (see earlier discussion).

Copine domains as protein-interacting modules

We identified CPNA-1 as an interacting partner for the giant polypeptide UNC-89, as well as for other M-line and dense body proteins. This interaction with UNC-89 is specific in two ways: 1) Only Ig domains 1–3, and not any of the other 50 Ig domains or any other segment of UNC-89, interact. 2) Only the copine domain of CPNA-1, and none of the copine domains from the six other copine domain-containing proteins in *C. elegans*, interacts with UNC-89.

Previous studies demonstrated that the copine domain is a protein–protein interacting domain (Hua *et al.*, 2001; Yang *et al.*, 2006; Li *et al.*, 2010). Tomsig *et al.* (2003) used the copine domains of three human copine proteins (copines I, II, and IV) to screen a mouse embryo two-hybrid library and identified

21 interacting proteins. The targets fell into several functional categories, including regulators of protein phosphorylation, transcription, or ubiquitination, calcium-binding proteins, and cytoskeletal or structural proteins. A majority of the interactors (14 of 21) contained predicted coiled-coil domains. CPNA-1 interactors are also regulators of phosphorylation (UNC-89 has two kinase domains and SCPL-1 is a phosphatase) and cytoskeletal proteins (PAT-6, LIM-9, and UNC-96). None of our interactors, however, contains predicted coiled-coil regions, and none of our proteins is a homologue of any proteins found by these authors. This is a further indication that the copine domain can interact with proteins of diverse functions.

Summary

We identified and characterized CPNA-1, a copine domain-containing protein required in *C. elegans* body-wall muscle during embryogenesis specifically for maintaining the structural integrity of the sarcomere. CPNA-1 is localized to integrin adhesion sites in muscle tissue and might act as a linker between membrane-proximal attachment proteins and those deeper within muscle cells. To date, this is the only copine domain-containing protein implicated in muscle maintenance/stability. Given that there are copine homologues in a diverse range of species including humans, further study on copines in other species is needed to determine whether this muscle function of copine domain containing proteins is evolutionarily conserved.

MATERIALS AND METHODS

Strains used

N2 (Bristol) is the primary wild-type strain used for *C. elegans* research, and standard growth conditions were used (Brenner, 1974). VC516 *cpna-1(gk266)/mIn1[mIs14 dpy-10(e128)] II* contains a deletion in *cpna-1*, and VC209 *lim-9(gk106) I* and VC349 *lim-9(gk210) I* carry mutations in the gene *lim-9*. Each was provided by the International *C. elegans* Gene Knockout Consortium (Vancouver, Canada). DM7439 *ex217* was created by transforming wild-type worms with the YFP-recombineered fosmid fDM1217, and the strain DM5151 *cpna-1(gk266)/+; ex217* was created by crossing in the *gk266* allele from strain VC516. Strain WB201 *pat-4(st587) III; ex(pat-4::GFP/pat-3::YFP)* was provided by Ben Williams (University of Illinois, Urbana, IL). Strains RW3600 *pat-3(st564)/qC1 dpy-19(e1259) glp-1(q339) III* and RW3568 *pat-6(st561)/dpy-9(e12) IV* were provided by Robert Waterston (University of Washington, Seattle, WA), and RW1596 *myo-3(st386) V; stEx30* was provided by Pam Hoppe (Western Michigan University). Strain GB244 *unc-96(sf18) X* was generated in the Benian lab (Mercer *et al.*, 2006). Strain HE75 *unc-89(su75) I* was provided by Henry Epstein (University of Texas Medical Branch at Galveston, Galveston, TX).

pat-6 (RNAi)

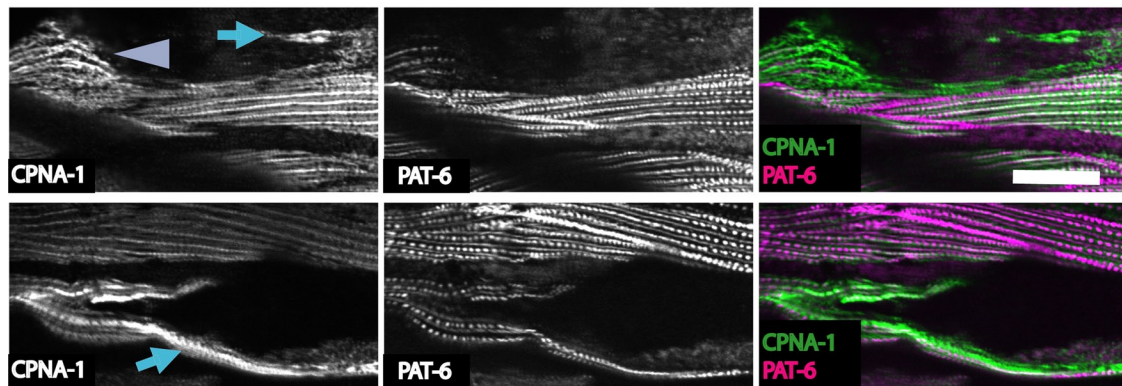


FIGURE 8: In adult muscle, PAT-6 is required for localization of CPNA-1. RNAi was used to knock down *pat-6* beginning at the L1 larval stage, and the resulting adults were immunostained for PAT-6 and CPNA-1. Top and bottom, portions of body-wall muscle from two such animals. In muscle cells in which PAT-6 was knocked down, CPNA-1 is found in abnormal accumulations (arrowhead) or mislocalized to the edge of the muscle cell near the muscle cell membrane (arrows). Bar, 10 μ m.

Screening of yeast two-hybrid library

Two-hybrid screening was performed as described in Miller *et al.* (2006). The first screen of the RB2 library of *C. elegans* random primed cDNAs (kindly provided by Robert Barstead, Oklahoma Medical Research Foundation, Oklahoma City, OK) used the bait plasmid pGBDU-UNC-89 GX34, which contains coding sequence for UNC-89 Ig1–5. To make the Ig1–5 bait, an insert generated by PCR using primers GX3 with added *Bam*HI site and GX4 with added *Xho*I site was ligated into pGBDU-C1 (see Supplemental Table S2 for primer sequences). From a screen of 819,500 colonies, the following prey clones were isolated: 35 preys representing VIG-1, 1 prey from UNC-54 (residues 1–602), 1 prey from KETN-1 (residues 4394–4889), and 1 prey from CPNA-1 (called GX9-109, residues 173–1107). A second screen of the library used a bait plasmid that contains coding sequence for UNC-89 Ig2–5. This bait was generated by insertion of a PCR fragment using primers GX2/5 with added *Bam*HI site and GX4. From a screen of 1,206,000 colonies, the following prey clones were isolated: 4 preys from VIG-1, 1 prey from UNC-54 (residues 1–602), 1 prey from MEL-26 (residues 25–343), and 1 prey from CPNA-1 (called B15-101, residues 825–1058). Interaction with VIG-1 was not pursued because it is part of a RISC complex (Caudy *et al.*, 2003) and thus we believed that this did not make biological sense. We did not pursue interaction with UNC-54 (myosin heavy chain B), which is located in the polar regions of the A-band (Miller *et al.*, 1983) rather than at the M-line where UNC-89 is located. Similarly, interaction with KETN-1 was not pursued, as KETN-1 is located in the I-band/dense body region of the sarcomere (Ono *et al.*, 2006). The interaction of UNC-89 and MEL-26 is described in Wilson *et al.* (2012).

Construction of two-hybrid clones covering all of UNC-89-B and its screening with CPNA-1

Seventeen segments (Figure 6B), covering all of UNC-89-B, were cloned into two-hybrid bait and prey vectors. Three of these segments were described previously: Fn1-Ig52-PK1 and Ig53-Fn2-PK2 (Qadota *et al.*, 2008b) and interkinase (Xiong *et al.*, 2009). For the other segments, corresponding cDNA fragments of UNC-89-B were amplified by using PCR with primers listed in Supplemental Table S2 and cloned into pBluescript. After confirming that the DNA sequence of each fragment was error-free, we cloned each fragment

into pGBDU or pGAD yeast two-hybrid plasmids. To screen for interaction with CPNA-1, first, PJ69-4A yeast host strains carrying each fragment of UNC-89-B in pGBDU were prepared, and then each strain was transformed with CPNA-1 prey clone B15-101 (residues 825–1058). The yeast two-hybrid assay was performed by scoring growth on media lacking histidine or adenine.

Screening of yeast two-hybrid bookshelf of known M-line and dense body proteins

CPNA-1 was used as both bait and prey to screen a collection ("bookshelf") of 23 known components of nematode M-lines and dense bodies (Supplemental Table S1). Both CPNA-1 (825–1058) and CPNA-1 (173–1107) were used.

Domain mapping of UNC-89 Ig1-5, SCPL-1, LIM-9, PAT-6, and UNC-96

To map the region of UNC-89 Ig1–5 minimally required for interaction with CPNA-1, we generated deletion derivatives of Ig1–5 by PCR using primers listed in Supplemental Tables S2 and S3. After cloning into pBluescript and identifying clones lacking PCR induced errors, we cloned the fragments into pGBDU and then tested them by two-hybrid assay against GX9-109 library prey clone CPNA-1 (173–1107). Domain mapping experiments reported in Figure 6, D–H, used constructs described previously: SCPL-1 (Qadota *et al.*, 2008b), LIM-9 (Qadota *et al.*, 2007), PAT-6 (Lin *et al.*, 2003), and UNC-96 (Mercer *et al.*, 2006; Qadota *et al.*, 2007). Derivatives of SCPL-1, LIM-9, and PAT-6 in pGAD were tested against CPNA-1 (173–1107) in pGBDU. Derivatives of UNC-96 in pGBDU were tested against CPNA-1 (825–1058) in pACT.

Testing for interaction of UNC-89 Ig1–5 against copine domains of other *C. elegans* proteins

To test the specificity of interaction between UNC-89 Ig 1–5 and the copine domain of CPNA-1, we generated the copine domains of other copine domain-containing proteins by PCR using the primers listed in Supplemental Table S3. The 5' primers have added *Bam*HI or *Sma*I sites, and the 3' primers have added *Xho*I sites. The products were ligated into pBluescript, sequenced, and then cloned into pGBDU and pGAD vectors. Yeast two-hybrid assays were performed by using pGAD copine domain clones against pGBDU UNC-89 Ig

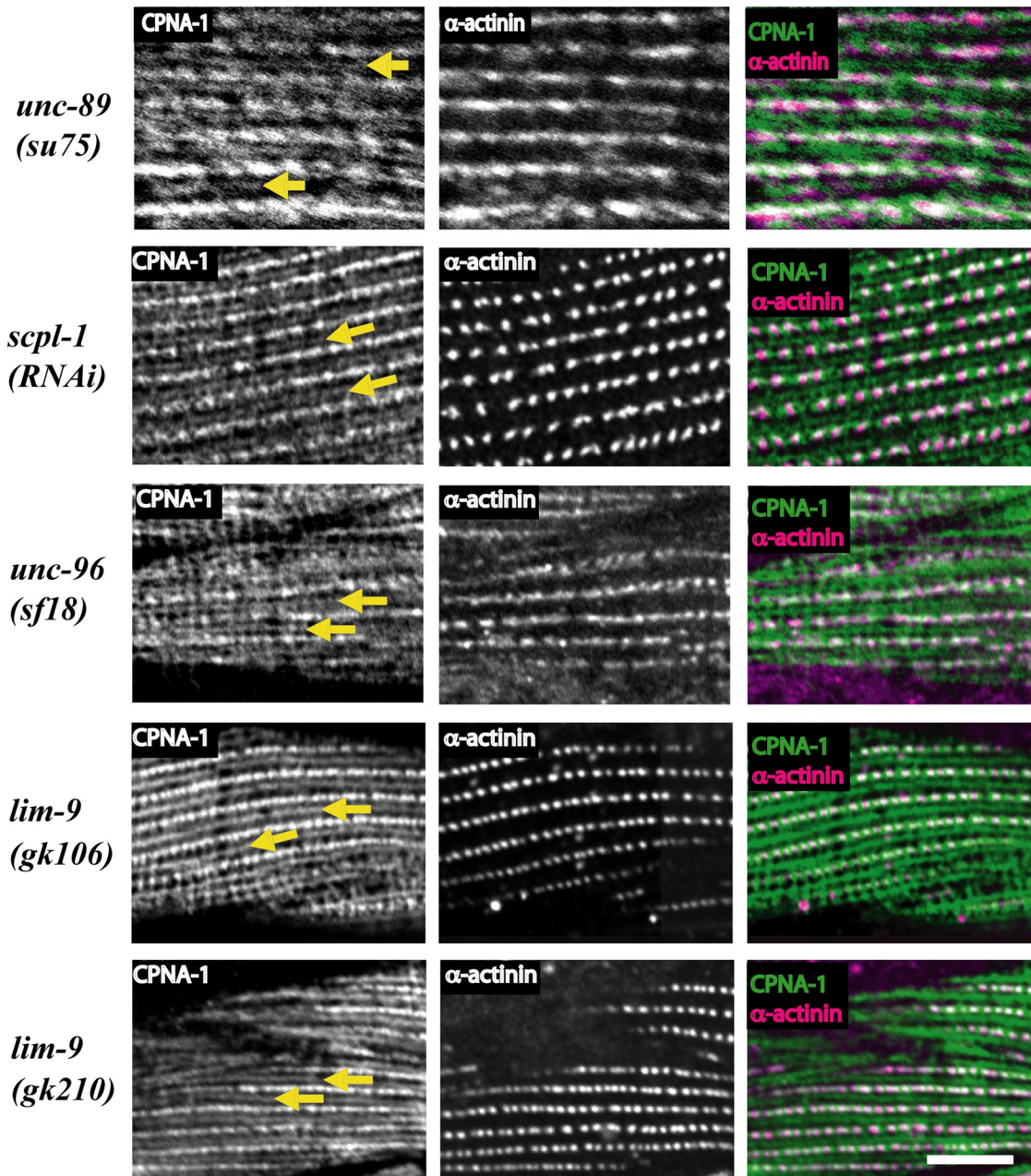


FIGURE 9: Analysis of mutants places the M-line proteins UNC-96, LIM-9, and SCPL-1 downstream of CPNA-1 in late larval or adult muscle. The indicated loss-of-function mutants or RNAi animals were coimmunostained with anti-CPNA-1 and anti- α -actinin. The localization of CPNA-1 at M-lines (indicated by yellow arrows) is unaffected by the absence or reduced levels of UNC-89, SCPL-1, UNC-96, or LIM-9. Note that the *unc-89*-mutant allele *su75*, which lacks all large UNC-89 isoforms, lacks CPNA-1-binding sites. Bar, 10 μ m.

1–5 yeast strain and pGBDU copine domain clones against the pGAD UNC-89 Ig1–5 clone, respectively. The results of both assays are consistent and are shown in Figure 2.

Testing for interaction of UNC-89 Ig1–5 and UNC-96 (201–418) against single-amino acid mutants of the copine domain of CPNA-1

To test whether the conserved amino acid residues within the copine domain of CPNA-1 are important for the binding with other proteins, we generated four point mutants using the primers listed in Supplemental Table S3 and used a method involving two rounds of PCR similar to that described in Qadota *et al.* (2012). Mutant

fragments were cloned into pGAD and tested against pGBDU UNC-89 Ig1–5 and pGBDU UNC-96 (201–418) yeast strains. Mutant fragments were also cloned into pGBDU and tested against pGAD UNC-89 Ig1–5 and pGAD UNC-96 (201–418).

Demonstration of interactions using purified proteins

To verify the interaction of CPNA-1 with UNC-89 Ig1–3, we pulled CPNA-1 out of a worm lysate using glutathione *S*-transferase (GST)–Ig1–3. To generate GST–Ig1–3, we excised the insert from pGBDU–Ig1–3 with *Bam*HI and *Bgl*II and cloned it into the *Bam*HI site of pGEX-KK1. After identifying a clone with the proper orientation, we prepared a GST fusion protein. Preparation of a *C. elegans* lysate

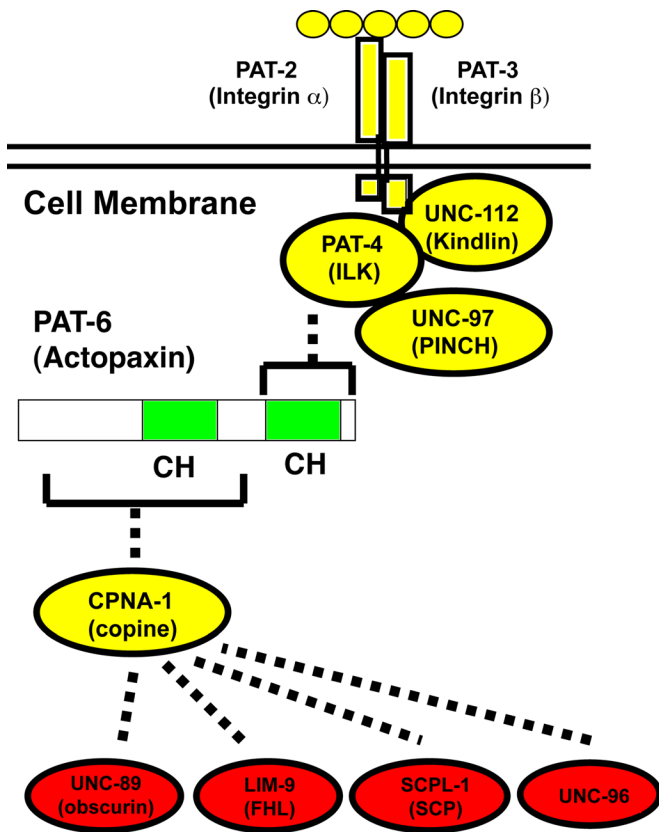


FIGURE 10: Model suggested by this study to explain the role of CPNA-1 in assembly of integrin adhesion complexes. UNC-112 (kindlin), PAT-4 (ILK), UNC-97 (PINCH), and PAT-6 (actopaxin) form a four-protein complex associated with the cytoplasmic tail of β -integrin. Lin *et al.* (2003) showed that the second CH domain of PAT-6 interacts with PAT-4. Here we show that PAT-6 (actopaxin) is needed to localize CPNA-1 to the muscle integrin adhesion complexes. CPNA-1, in turn, is needed for proper localization of UNC-89 (obscurin), LIM-9 (FHL), SCPL-1 (SCP), and UNC-96 to M-lines. We have not yet identified CPNA-1-interacting proteins that are specific for dense bodies. Yellow indicates proteins that are located at both M-lines and dense bodies and whose loss of function result in Pat embryonic lethality. Red indicates proteins that are located at M-lines and whose loss of function results in adult muscle phenotypes.

and the procedure used for pull down of CPNA-1 were as described in Qadota *et al.* (2012). An HA bead pull-down assay, performed essentially as described in Qadota *et al.* (2008a), was used to verify the interaction between CPNA-1 (825–1058) and UNC-96 (201–418). In this assay yeast was used to express HA-tagged CPNA-1 (copine), using primers listed in Supplemental Table S3. Construction and purification of maltose-binding protein (MBP)–UNC-96 (201–418) was described in Mercer *et al.* (2006). Far Western assays, performed essentially as described in Mercer *et al.* (2006), were used to verify the interactions between CPNA-1 and UNC-89 Ig1–3 and between CPNA-1 and SCPL-1, LIM-9, or PAT-6. To express MBP–CPNA-1 (825–1058), the B15-101 prey clone was digested with *Xho*I, and the insert was cloned into the *Xho*I site of pMAL-KK2. After identification of a clone with proper orientation, MBP–CPNA-1 (825–1058) was expressed and purified. To express hexahistidine (6His)–Ig1–3, pGBDU-Ig1–3 was digested with *Bam*HI and *Bgl*II, and the insert was ligated into pET28a. A clone with the proper orientation was used to produce 6His–Ig1–3. MBP–CPNA-1 (825–1058) was run on

SDS–PAGE, transferred to a blot, incubated with 6His–Ig1–3, and then detected with anti-His and anti-rabbit horseradish peroxidase (HRP). To express His–CPNA-1 (173–1107), pGBDU-CPNA-1 (173–1107) was digested with *Eco*RI (site in the vector) and *Sal*I (in the insert), and this fragment, encoding the N-terminal two-thirds of CPNA-1 (173–1107) was ligated into pET28a to create clone a. The C-terminal one third of CPNA-1 (173–1107) was generated by PCR using primers with added *Hind*III and *Xho*I sites, cloned into pBlue-script. After finding an error-free pBlue-script clone, we excised the insert with *Hind*III and *Xho*I and ligated it into pET28a. The resulting clone was digested with *Eco*RI (in the vector) and *Sal*I (in the CPNA-1 insert), and the large fragment containing mostly vector sequence and the 3' portion of the insert was ligated to insert of clone a previously digested with *Eco*RI and *Sal*I, to produce a plasmid that could produce His–CPNA-1 (173–1107). His–CPNA-1 (173–1107) was run on SDS–PAGE, transferred to a blot, incubated with either MBP–SCPL-1 (phosphatase domain; Qadota *et al.*, 2008b), MBP–PAT-6 (full length; Lin *et al.*, 2003), or MBP–LIM-9 (LIM domains; Qadota *et al.*, 2007), and then detected with anti-MBP–HRP. Procedures for growth of yeast for expressing HA-tagged proteins, growth of bacteria, and purification of GST-, MBP-, and His-tagged proteins were described previously (Mercer *et al.*, 2006; Qadota *et al.*, 2008a).

Generation of antibodies to CPNA-1

Residues 176–385 of CPNA-1b were expressed and purified in *Escherichia coli* as a GST fusion protein. To do this, primers tag-149-1 and tag-149-2 with added *Eco*RI and *Xho*I sites were used to create a PCR fragment using cDNA GX9-109 as template. This fragment was cloned into pBlue-script, and a clone without PCR-induced errors was used for excising the insert. This insert was ligated into pGEX-KK1 using the same enzyme sites. Using methods described in Mercer *et al.* (2006), we expressed GST–CPNA-1(176-385), purified it, and shipped it to Spring Valley Laboratories (Woodbine, MD) for generation of rabbit polyclonal antibodies. Most of the anti-GST antibodies were removed by immunoprecipitation using GST, and anti–CPNA-1 was affinity purified using Affi-Gel conjugated with GST–CPNA-1(176-385), as described previously (Mercer *et al.*, 2003). These antibodies detect a band of expected size on Western blot (Supplemental Figure S1) and react to wild-type but not *cpna-1*–null embryos on immunostaining.

Western blots

The procedure of Hannak *et al.* (2002) was used to prepare total protein lysates from wild-type animals and from worms that had undergone *pat-6(RNAi)* by L1 feeding (Miller *et al.*, 2006). Approximately 50–100 μ g of total protein was separated by a 10% SDS–PAGE, transferred to nitrocellulose membrane, and reacted with affinity purified and OP50 *E. coli* absorbed anti–CPNA-1 at 1:100 or 1:500 dilution, or affinity-purified and OP50 *E. coli* absorbed anti–PAT-6 at 1:200 dilution, followed by reaction with appropriate HRP-conjugated secondary antibodies and visualization using enhanced chemiluminescence (cat. no. 32106; Pierce, Rockford, IL).

Immunolocalization in adult body-wall muscle

Worms were fixed by the Nonet method (Nonet *et al.*, 1993), with the exception of Figure 3A (third row), in which strain DM5115 (UNC-112::GFP), which was fixed using the constant-spring method (Benian *et al.*, 1996). Primary antibodies were used at the following dilutions: anti–CPNA-1 at 1:100, anti–UNC-89 (monoclonal MH42; Benian *et al.*, 1996) at 1:200, anti– α -actinin (MH35; Francis and Waterston, 1991) at 1:200, anti–myosin heavy chain A (MHC A; 5-6;

Miller et al., 1983) at 1:200, and anti-PAT-6 at 1:100. For anti-CPNA-1, the secondary was anti-rabbit conjugated to Alexa 488 (the one exception was when DM5115 was stained; then we used anti-rabbit Cy3); for the monoclonals (MH35, MH42, and 5-6) the secondary was anti-mouse-Alexa 594; and for anti-PAT-6, we used anti-rat-Alexa 594. Images were captured at room temperature with a Zeiss confocal system (LSM510; Zeiss, Jena, Germany) equipped with an Axiovert 100M microscope using an Aplanachromat 63×/1.4 oil objective in 2.5× zoom mode. The color balances of the images were adjusted with Photoshop (Adobe, San Jose, CA).

RNAi

RNAi of *pat-6* was performed by feeding wild-type strain N2 worms bacteria expressing double-stranded RNA beginning at the L1 larval stage and continuing until the animals reached adulthood. Adults were then fixed and immunostained (Miller et al., 2006).

Generation and characterization of antibodies to PAT-6

Residues 1–99 of PAT-6 were expressed in *E. coli* and purified as a GST fusion protein. Primers PAT-6-1 and PAT-6-99 with added *Bam*HI and *Xho*I sites were used to amplify a fragment from the full-length clone of *pat-6* in the two-hybrid bait vector. The resulting fragment was cloned directly into *Bam*HI- and *Xho*I-cut pGEX-KK1. After identification of a clone with an error-free insert, the clone was used to produce GST-PAT-6(1-99). This protein was shipped to Spring Valley Laboratories for generation of polyclonal antibodies in rats. Affinity purification was performed using Affigel conjugated to GST-PAT-6(1-99). Western blot extracts, as described earlier, were prepared from adults that had been subjected to RNAi by feeding beginning at the L1 stage, either with bacteria containing the empty vector or *pat-6* cDNA sequence, and subjected to Western blot analysis using anti-PAT-6 (see Supplemental Figure S5). Wild-type adult muscle was costained with anti-CPNA-1 and anti-PAT-6 and imaged as described.

Immunostaining of embryonic muscle

Antibody staining of *C. elegans* embryos was carried out using a method modified from Albertson (1984). Adult worms were washed off plates and incubated for 5 min in embryo preparation solution containing 75% distilled H₂O, 20% sodium hypochlorite, and 5% 10 M NaOH to dissolve the adult worm cuticles. After spinning down of the suspension, the remaining embryos and worm carcasses were incubated for another 2 min in the embryo preparation solution, followed by three washes in M9 buffer. The remaining embryos were then either suspended in a 4% sucrose and 1 mM EDTA, pH 7.4, solution or left to incubate for 6 h to obtain later-stage embryos before resuspension. The egg suspension was transferred to glass slides coated with 2 mg/ml poly-L-lysine, covered by a rectangular glass coverslip, and frozen on an aluminum slab at –80°C overnight. The coverslips were removed from the slides using a razor blade, and slides were transferred to –20°C acetone for 4 min, with subsequent 1-min intervals of 75% acetone at 20°C, 50% acetone, 25% acetone, and Tween-TBS for 2 min. Embryos were double stained with anti-CPNA-1 together with antibodies to the various integrin adhesion complex proteins indicated in Figure 4. The double staining allowed identification of *cpna-1*-null embryos among the progeny of *cpna-1*/*+* parental worms. Primary antibodies solutions were added to the slides for 5 h and included anti-CPNA-1 (rabbit) at 1:100 together with anti-PAT-3 (mouse MH25; Francis and Waterston, 1985) at 1:500, anti-DEB-1 (vinculin; mouse MH24; Francis and Waterston, 1985) at 1:250, anti-PAT-6 (rat) at 1:40, or anti MYO-3 (mouse DM5-6; Miller et al., 1983) at 1:250 dilutions. It

was not possible to double stain with anti-CPNA-1 and anti-PAT-4, as both are rabbit antibodies. However, none of the embryos from *cpna-1*/*+* parents showed mislocalization of PAT-4 (anti-PAT-4 used at 1:40 dilution). After incubation, slides were washed for 1 h in TBS-Tween and then removed and coated with secondary antibodies for 3 h: anti-rabbit Alexa 488 (Invitrogen, Carlsbad, CA) for PAT-4 and CPNA-1 antibodies, anti-mouse Alexa 594 (Invitrogen) for MH25, MH24, and DM5-6, and anti-rat Alexa 594 (Invitrogen) for anti-PAT-6. After a 1 h wash in TBS-Tween, mounting solution was added (20 mM Tris, pH 8.0, 0.2 M DABCO, and 90% glycerol) and slides were sealed with nail polish.

Generation of a translational YFP fusion for *cpna-1*

A C-terminal YFP translational fusion construct was created for *cpna-1* using the fosmid recombineering method described in Tursun et al. (2009). The recombineered fosmid was named fDM1217, and a solution containing 94 ng/μl pRF4 *rol-6*(*su1006dm*) and 6 ng/μl fDM1217 was injected into the gonad of adult N2 animals using conventional methods as described in Mello et al. (1991).

Electron microscopy

For noncolloidal gold electron microscopy (EM), fixation and imaging was carried out identically to the procedure outlined in Warner et al. (2011). For colloidal gold EM, CPNA-1::YFP worms were transferred from agar plates and immersed in fixative. Under a dissecting microscope, worms were cut in half using a scalpel and collected in a vial. The fixation protocol used was a two-step method described in detail elsewhere (Vaid et al., 2007). Worms were embedded in Lowicryl, sectioned, placed on Formvar/carbon-coated grids, phosphate-buffered saline (PBS)/0.1% bovine serum albumin (BSA)/0.5% Tween 20/1:20 normal goat serum (NGS) was aliquoted onto Parafilm in 8-μl drops, and grids were placed face down onto drops for 5 min. Primary chicken anti-GFP antibody (13970; Abcam, Cambridge, MA; also reacts with YFP) was diluted in PBS/0.1% BSA/0.5% Tween 20/1% NGS at a 1:1000 dilution, and 8 μl per grid (grids placed face down on drops) was used for an overnight incubation. Grids were then washed three times with PBS/0.1% BSA/ 0.05% Tween 20 (grids placed face down on drops). The secondary rabbit polyclonal anti chicken IgY antibody conjugated with 10 nm colloidal gold (39612; Abcam) was diluted 1:200 in PBS/0.1% BSA/ 0.05% Tween 20/ 5.0% fetal bovine serum (FBS), with the solution diluted 1:20 prior to antibody addition. The secondary antibody solution was aliquoted into 8 μl drops, and grids were placed face down for 2 h. Controls were incubated solely with either secondary antibody without primary, or chicken IgY (119138; Abcam) followed by secondary antibody incubation. Grids were then washed twice with PBS using hanging drops, then fixed for 10 min with 1% glutaraldehyde in PBS. Grids were then washed twice with distilled water using hanging drops, incubated on 8 μl drops of uranyl acetate for 3 min, then washed three times with distilled water, dried, and stored in a dessicator prior to imaging. Imaging was carried out using a Tecnai G2 Spirit electron microscope (FEI, Hillsboro, OR) operated at 120 kV. Quantification of gold particle localization was carried out by counting the number of gold particles in a region of 100 nm centered about a dense body. Four control sections and four colloidal gold-labeled CPNA-1 sections were utilized.

Yeast three-hybrid assay

The yeast three-hybrid assay was done essentially as described in Lin et al. (2003).

Sequence analysis

BLAST, using CPNA-1 as query against the *C. elegans* translated genome, was used to identify the complete set of copine containing proteins in this organism, as well as those in other organisms. PFAM was used to identify the copine domain boundaries and to identify other possible domains (e.g., C2 domains). The multisequence alignment of copine domains from *C. elegans* was performed using www.genome.jp/tools/clustalw/. To predict possible transmembrane helices in the copine family, we used the following programs: TMHMM Server v. 2.0 (www.cbs.dtu.dk/services/TMHMM-2.0), PRED-TMR (<http://athina.biol.uoa.gr/PRED-TMR/input.html>), and HMMtop (www.enzim.hu/hmmtop/server/hmmtop.cgi).

ACKNOWLEDGMENTS

We thank Kim M. Gernert (Emory University, Atlanta, GA) for help in predicting the transmembrane domain of CPNA-1. We also thank Pamela Hoppe (Western Michigan University, Kalamazoo, MI) for her help editing the manuscript. G.M.B. thanks the Department of Pathology, Emory University, for current support, and the National Institutes of Health for previous support (Grants AR051466 and AR052133). D.G.M. thanks the Canadian Institute for Health Research and the National Science and Engineering Research Council of Canada for current support. D.G.M. is a Canadian Institute for Advanced Research Fellow.

REFERENCES

- Albertson DG (1984). Formation of the first cleavage spindle in nematode embryos. *Dev Biol* 101, 61–72.
- Bang ML et al. (2001). The complete gene sequence of titin, expression of an unusual approximately 700-kDa titin isoform, and its interaction with obscurin identify a novel Z-line to I-band linking system. *Circ Res* 89, 1065–1072.
- Barstead RJ, Waterston RH (1991). Vinculin is essential for muscle function in the nematode. *J Cell Biol* 114, 715–724.
- Benian GM, Ayme-Southgate A, Tinley TL (1999). The genetics and molecular biology of the titin/connectin-like proteins of invertebrates. *Rev Physiol Biochem Pharmacol* 138, 235–268.
- Benian GM, Tinley TL, Tang X, Borodovsky M (1996). The *Caenorhabditis elegans* gene *unc-89*, required for muscle M-line assembly, encodes a giant modular protein composed of Ig and signal transduction domains. *J Cell Biol* 132, 835–848.
- Brenner S (1974). The genetics of *Caenorhabditis elegans*. *Genetics* 77, 71–94.
- Caudy AA, Ketting RF, Hammond SM, Denli AM, Bathoorn AM, Tops BB, Silva JM, Myers MM, Hannon GJ, Plasterk RH (2003). A micrococcal nuclease homologue in RNAi effector complexes. *Nature* 425, 411–414.
- Church DL, Lambie EJ (2003). The promotion of gonadal cell divisions by the *Caenorhabditis elegans* TRPM cation channel GON-2 is antagonized by GEM-4 copine. *Genetics* 165, 563–574.
- Cox EA, Hardin J (2004). Sticky worms: adhesion complexes in *C. elegans*. *J Cell Sci* 117, 1885–1897.
- Creutz CE, Tomsig JL, Snyder SL, Gautier MC, Skouri F, Beisson J, Cohen J (1998). The copines, a novel class of C2 domain-containing, calcium-dependent, phospholipid-binding proteins conserved from *Paramecium* to humans. *J Biol Chem* 273, 1393–1402.
- Damer CK, Bayeva M, Kim PS, Ho LK, Eberhardt ES, Socec CI, Lee JS, Bruce EA, Goldman-Yassen AE, Naliboff LC (2007). Copine A is required for cytokinesis, contractile vacuole function, and development in *Dictyostelium*. *Eukaryot Cell* 6, 430–442.
- Ferrara TM, Flaherty DB, Benian GM (2005). Titin/connectin-related proteins in *C. elegans*: a review and new findings. *J Muscle Res Cell Motil* 26, 435–447.
- Epstein HF, Waterston RH, Brenner S (1974). A mutant affecting the heavy chain of myosin in *Caenorhabditis elegans*. *J Mol Biol* 90, 291–300.
- Francis GR, Waterston RH (1985). Muscle organization in *Caenorhabditis elegans*: localization of proteins implicated in thin filament attachment and I-band organization. *J Cell Biol* 101, 1532–1549.
- Francis R, Waterston RH (1991). Muscle cell attachment in *Caenorhabditis elegans*. *J Cell Biol* 114, 465–479.
- Gettner SN, Kenyon C, Reichardt LF (1995). Characterization of beta pat-3 heterodimers, a family of essential integrin receptors in *C. elegans*. *J Cell Biol* 129, 1127–1141.
- Gottschalk A, Almedom RB, Schedletzky T, Anderson SD, Yates JR 3rd, Schafer WR (2005). Identification and characterization of novel nicotinic receptor-associated proteins in *Caenorhabditis elegans*. *EMBO J* 24, 2566–2578.
- Hannak E, Oegema K, Kirkham M, Gonczy P, Habermann B, Hyman AA (2002). The kinetically dominant assembly pathway for centrosomal asters in *Caenorhabditis elegans* is gamma-tubulin dependent. *J Cell Biol* 157, 591–602.
- Hoebert O, Moerman DG, Clark KA, Beckerle MC, Ruvkun G (1999). A conserved LIM protein that affects muscular adhesion junction integrity and mechanosensory function in *Caenorhabditis elegans*. *J Cell Biol* 144, 45–57.
- Hua J, Grisafi P, Cheng SH, Fink GR (2001). Plant growth homeostasis is controlled by the *Arabidopsis* BON1 and BAP1 genes. *Genes Dev* 15, 2263–2272.
- Jambunathan N, Siani JM, McNellis TW (2001). A humidity-sensitive *Arabidopsis* copine mutant exhibits precocious cell death and increased disease resistance. *Plant Cell* 13, 2225–2240.
- Kontogianni-Konstantopoulos A, Ackermann MA, Bowman AL, Yap SV, Bloch RJ (2009). Muscle giants: molecular scaffolds in sarcomerogenesis. *Physiol Rev* 89, 1217–1267.
- Krogh A, Larsson B, von Heijne G, Sonnhammer ELL (2001). Predicting transmembrane protein topology with a hidden Markov model: application to complete genomes. *J Mol Biol* 305, 567–580.
- Larkin MA et al. (2007). Clustal W and Clustal X version 2.0. *Bioinformatics* 23, 2947–2948.
- Lee JO, Rieu P, Arnaout MA, Liddington R (1995). Crystal structure of the A domain from the alpha subunit of integrin CR3 (CD11b/CD18). *Cell* 80, 631–638.
- Li Y, Gou M, Sun Q, Hua J (2010). Requirement of calcium binding, myristoylation, and protein-protein interaction for the Copine BON1 function in *Arabidopsis*. *J Biol Chem* 285, 29884–29891.
- Lin X, Qadota H, Moerman DG, Williams BD (2003). *C. elegans* PAT-6/actopaxin plays a critical role in the assembly of integrin adhesion complexes in vivo. *Curr Biol* 13, 922–932.
- Mackinnon AC, Qadota H, Norman KR, Moerman DG, Williams BD (2002). *C. elegans* PAT-4/ILK functions as an adaptor protein within integrin adhesion complexes. *Curr Biol* 12, 787–797.
- Meissner B et al. (2009). An integrated strategy to study muscle development and myofibrillar structure in *Caenorhabditis elegans*. *PLoS Genet* 5, e1000537.
- Meissner B, Rogalski T, Viveiros R, Warner A, Plastino L, Lorch A, Granger L, Segalat L, Moerman DG (2011). Determining the sub-cellular localization of proteins within *C. elegans* body wall muscle. *PLoS ONE* 6, e19937.
- Mello CC, Kramer JM, Stinchcomb D, Ambros V (1991). Efficient gene transfer in *C. elegans*: extrachromosomal maintenance and integration of transforming sequences. *EMBO J* 10, 3959–3970.
- Mercer KB, Flaherty DB, Miller RK, Qadota H, Tinley TL, Moerman DG, Benian GM (2003). *Caenorhabditis elegans* UNC-98, a C2H2 Zn finger protein, is a novel partner of UNC-97/PINCH in muscle adhesion complexes. *Mol Biol Cell* 14, 2492–2507.
- Mercer KB, Miller RK, Tinley TL, Sheth S, Qadota H, Benian GM (2006). *Caenorhabditis elegans* UNC-96 is a new component of M-lines that interacts with UNC-98 and paramyosin and is required in adult muscle for assembly and/or maintenance of thick filaments. *Mol Biol Cell* 17, 3832–3847.
- Miller DM 3rd, Ortiz I, Berliner GC, Epstein HF (1983). Differential localization of two myosins within nematode thick filaments. *Cell* 34, 477–490.
- Miller RK, Qadota H, Landsverk ML, Mercer KB, Epstein HF, Benian GM (2006). UNC-98 links an integrin-associated complex to thick filaments in *Caenorhabditis elegans* muscle. *J Cell Biol* 175, 853–859.
- Moerman DG, Fire A (1997). Muscle structure, function and development. In: *C. elegans II/D*, ed. L Riddle, T Blumenthal, BJ Meyer, JR Priess, Plainview, NY: Cold Spring Harbor Laboratory Press, 417–470.
- Moerman DG, Williams BD (2006). Sarcomere assembly in *C. elegans* muscle. In: *WormBook*, ed. The *C. elegans* Research Community, doi/10.1895/wormbook.1891.1881.1891.
- Nahabedian JF, Qadota H, Stirman JN, Lu H, Benian GM (2011). Bending amplitude—a new quantitative assay of *C. elegans* locomotion: identification of phenotypes for mutants in genes encoding muscle focal adhesion components. *Methods* 56, 95–102.

- Nonet ML, Grundahl K, Meyer BJ, Rand JB (1993). Synaptic function is impaired but not eliminated in *C. elegans* mutants lacking synaptotagmin. *Cell* 73, 1291–1305.
- Norman KR, Cordes S, Qadota H, Rahmani P, Moerman DG (2007). UNC-97/PINCH is involved in the assembly of integrin cell adhesion complexes in *Caenorhabditis elegans* body-wall muscle. *Dev Biol* 309, 45–55.
- Ono K, Yu R, Mohri K, Ono S (2006). *Caenorhabditis elegans* kettin, a large immunoglobulin-like repeat protein, binds to filamentous actin and provides mechanical stability to the contractile apparatuses in body-wall muscle. *Mol Biol Cell* 17, 2722–2734.
- Qadota H, Blangy A, Xiong G, Benian GM (2008a). The DH-PH region of the giant protein UNC-89 activates RHO-1 GTPase in *Caenorhabditis elegans* body-wall muscle. *J Mol Biol* 383, 747–752.
- Qadota H, McGaha LA, Mercer KB, Stark TJ, Ferrara TM, Benian GM (2008b). A novel protein phosphatase is a binding partner for the protein kinase domains of UNC-89 (obscurin) in *Caenorhabditis elegans*. *Mol Biol Cell* 19, 2424–2432.
- Qadota H, Mercer KB, Miller RK, Kaibuchi K, Benian GM (2007). Two LIM domain proteins and UNC-96 link UNC-97/pinch to myosin thick filaments in *Caenorhabditis elegans* muscle. *Mol Biol Cell* 18, 4317–4326.
- Qadota H, Moerman DG, Benian GM (2012). A molecular mechanism for the requirement of PAT-4 (ILK) for the localization of UNC-112 (kindlin) to integrin adhesion sites. *J Biol Chem* 287, 28537–28551.
- Rogalski TM, Mullen GP, Gilbert MM, Williams BD, Moerman DG (2000). The UNC-112 gene in *Caenorhabditis elegans* encodes a novel component of cell-matrix adhesion structures required for integrin localization in the muscle cell membrane. *J Cell Biol* 150, 253–264.
- Small TM, Gernert KM, Flaherty DB, Mercer KB, Borodovsky M, Benian GM (2004). Three new isoforms of *Caenorhabditis elegans* UNC-89 containing MLCK-like protein kinase domains. *J Mol Biol* 342, 91–108.
- Sonnhammer ELL, von Heijne G, Krogh A (1998). A hidden Markov model for predicting transmembrane helices in protein sequences. In: *Proceedings of the Sixth International Conference on Intelligent Systems for Molecular Biology*, ed. J Glasgow, T Littlejohn, F Major, R Lathrop, D Sankoff, and C Sensen, Menlo Park, CA: AAAI Press, 175–182.
- Tomsig JL, Creutz CE (2002). Copines: a ubiquitous family of Ca²⁺-dependent phospholipid-binding proteins. *Cell Mol Life Sci* 59, 1467–1477.
- Tomsig JL, Snyder SL, Creutz CE (2003). Identification of targets for calcium signaling through the copine family of proteins. Characterization of a coiled-coil copine-binding motif. *J Biol Chem* 278, 10048–10054.
- Tursun B, Cochella L, Carrera I, Hobert O (2009). A toolkit and robust pipeline for the generation of fosmid-based reporter genes in *C. elegans*. *PLoS One* 4, e4625.
- Vaid KS, Guttman JA, Babyak N, Deng W, McNiven MA, Mochizuki N, Finlay BB, Vogl AW (2007). The role of dynamin 3 in the testis. *J Cell Physiol* 210, 644–654.
- Warner A, Qadota H, Benian GM, Vogl AW, Moerman DG (2011). The *Caenorhabditis elegans* paxillin orthologue, PXL-1, is required for pharyngeal muscle contraction and for viability. *Mol Biol Cell* 22, 2551–2563.
- Waterston RH, Thomson JN, Brenner S (1980). Mutants with altered muscle structure of *Caenorhabditis elegans*. *Dev Biol* 77, 271–302.
- Waterston RH (1988). Muscle. In: *The Nematode Caenorhabditis elegans*, ed. WB Wood, Plainview, NY: Cold Spring Harbor Laboratory Press, 281–335.
- Whittaker CA, Hynes RO (2002). Distribution and evolution of von Willebrand/integrin A domains: widely dispersed domains with roles in cell adhesion and elsewhere. *Mol Biol Cell* 13, 3369–3387.
- Williams BD, Waterston RH (1994). Genes critical for muscle development and function in *Caenorhabditis elegans* identified through lethal mutations. *J Cell Biol* 124, 475–490.
- Wilson KJ, Qadota H, Mains PE, Benian GM (2012). UNC-89 (obscurin) binds to MEL-26, a BTB-domain protein, and affects the function of MEI-1 (katanin) in striated muscle of *Caenorhabditis elegans*. *Mol Biol Cell* 23, 2623–2634.
- Xiong G, Qadota H, Mercer KB, McGaha LA, Oberhauser AF, Benian GM (2009). A LIM-9 (FHL)/SCPL-1 (SCP) complex interacts with the C-terminal protein kinase regions of UNC-89 (obscurin) in *Caenorhabditis elegans* muscle. *J Mol Biol* 386, 976–988.
- Yang H, Li Y, Hua J (2006). The C2 domain protein BAP1 negatively regulates defense responses in *Arabidopsis*. *Plant J* 48, 238–248.
- Young P, Ehler E, Gautel M (2001). Obscurin, a giant sarcomeric Rho guanine nucleotide exchange factor protein involved in sarcomere assembly. *J Cell Biol* 154, 123–136.
- Zengel JM, Epstein HF (1980). Identification of genetic elements associated with muscle structure in the nematode *Caenorhabditis elegans*. *Cell Motil* 1, 73–97.